A Simplified Stator Frequency and Power Control Method of DFIG-DC System Without Stator Voltage and Current Sensors

Wu, Chao; Jiao, Yingzong; Nian, Heng; Blaabjerg, Frede

Published in:
I E E E Transactions on Power Electronics

DOI (link to publication from Publisher):
10.1109/TPEL.2019.2953677

Publication date:
2020

Document Version
Accepted author manuscript, peer reviewed version

Citation for published version (APA):
Wu, C., Jiao, Y., Nian, H., & Blaabjerg, F. (2020). A Simplified Stator Frequency and Power Control Method of DFIG-DC System Without Stator Voltage and Current Sensors. *I E E E Transactions on Power Electronics*, *35*(6), 5562-5566. [8907439]. https://doi.org/10.1109/TPEL.2019.2953677

This article has been accepted for publication in a future issue of this journal, but has not been fully edited. Content may change prior to final publication. Citation information: DOI 10.1109/TPEL.2019.2953677, IEEE Transactions on Power Electronics

A Simplified Stator Frequency and Power Control Method of DFIG-DC System Without Stator Voltage and Current Sensors

Chao Wu, Yingzong Jiao, Heng Nian, *Senior Member, IEEE* and Frede Blaabjerg, *Fellow, IEEE*

***Abstract*—The primary objective of the grid connected DFIG-DC system is to achieve the accurate control of stator frequency and active power. In this letter, a simplified power control method is proposed by just controlling the magnitude of the rotor current vector, which can avoid the stator voltage and current sensors. The stator active power is calculated by the product of dc voltage and dc current. The stator frequency is simply controlled by the rotating speed of the rotor current vector which is achieved through a given rotating frame. Furthermore, the parameter dependency and dc sampling offset problems can be eliminated because the voltage model or current model which are usually used for acquiring stator frequency and stator flux angle can be avoided. Therefore, the robustness and stability of the stator frequency and power control can be improved. Finally, experiments based on a 1 kW DFIG-DC setup is carried out to verify the proposed method.**

***Index Terms*— Doubly-fed induction generator, simplified stator frequency and power control, reduced sensors, robustness**

I. INTRODUCTION

Recently, a DFIG-DC topology, in which the DFIG is connected to the dc grid just by one rotor side converter (RSC) and one diode bridge on the stator side, has been extensively studied since the cost is greatly reduced and the configuration is simpler compared with other topologies [1]-[4]. However, due to the stator side diode bridge, the conventional decoupling power control strategy applied in the ac grid connected mode is not suitable in this DFIG-DC topology [5] and the stator frequency needs to be controlled additionally.

Some literatures have aimed at the decoupling control of stator frequency and stator power, which are mainly based on stator flux orientation method. In [6]-[8], the stator frequency and stator flux angle are calculated based on integrating the stator voltage which will introduce a dc sampling offset problem. In [9]-[11], the angle of stator flux is obtained based on current model which will cause parameter dependence on the inductance. In conclusion, no matter whether the voltage model or current model is applied to obtain the angle of stator flux, the stator voltage sensors or stator current sensors are essential. In [12], a stator side sensorless control method is proposed by estimating the stator current based on rotor current and dc voltage, which is also highly dependent on the DFIG parameters. Furthermore, this method can just be applied in the standalone mode which is not suitable for the grid connected mode since the control objective is the output power instead of the dc voltage. Furthermore, in [13], the stator voltage sensorless control method is proposed with stator current sensors, and also a rotor current sensorless method is proposed in [14], while stator voltage and current sensors are still necessary.

In this letter, a simplified stator frequency and power control method is proposed to avoid the stator voltage and current sensors. The stator power is controlled by the magnitude of rotor current vector and the stator frequency is controlled by the rotating speed of rotor current vector，which can be directly given. The orientation on the rotor current is achieved by controlling the *q*-axis rotor current to be zero. The advantages of this simplified power control method are:

1. Since the orientation angle is directly generated by the integral of stator frequency, the voltage model or current model which is used to obtain the orientation angle can be avoided. Thus, the stator voltage and current sensors can both be eliminated.
2. The problems of the parameter dependency and dc sampling offset question are solved, since there is no need to calculate the stator frequency and stator flux angle.
3. The effect of stator frequency control loop on power control loop is eliminated, thus, the stability of both stator frequency and power control loop are improved.

II. TOPOLOGY AND CONTROL SCHEME

In DFIG-DC system, the DFIG is working as power source to provide active power to dc grid according to wind speed. Thus, the control objective of the DFIG-DC system is the accurate control of power and stator frequency. The DFIG-DC topology and the RSC control scheme for the power and stator frequency are shown as Fig. 1. The dc voltage is sampled as V_{dc} and the dc current at stator side is sampled as I_{dcs}, the rotor currents $\boldsymbol{I}_{rabc}$ and rotor position θ_r are sampled for the RSC control. The stator frequency ω_s is directly given and the orientation angle is the integral of stator frequency. The stator active power is controlled through the magnitude of the rotor current vector.

A. Stator frequency Control

In steady state, the stator frequency is equal to the rotating speed of the rotor current vector in the stationary frame, which is directly given as ω_s. The angle of the synchronous *d*-*q* frame is the integral of stator frequency ω_s. Knowing the rotor angle θ_r and the angle of synchronous *d*-*q* frame, the slip angle of the generator can be calculated as,

$$\theta_{slip} = \frac{1}{s}\omega_s - \theta_r \tag{1}$$

The *q*-axis rotor current is controlled to zero to achieve the rotor current orientation control. Thus, the reference of *q*-axis rotor current is zero, which can be seen from Fig. 1.

B. *Output power control*

The stator active power can be calculated by the dc voltage and dc current at stator side as,

$$P_s = V_{dc} \cdot I_{dcs} \tag{2}$$

Since the stator active power has a positive correlation with the magnitude of rotor current, the power can be regulated through the magnitude of rotor current. If the rotor current orientation control is achieved, the magnitude of the rotor current is equal to *d*-axis rotor current. Thus, the generation of *d*-axis rotor current reference can be expressed as,

$$I_{rd}^{*} = \frac{k_{pp}s + k_{ip}}{s}\left(P_s^{*} - P_s\right) \tag{3}$$

where k_{pp} and k_{ip} are the proportional gain and integral gain of the power loop controller.

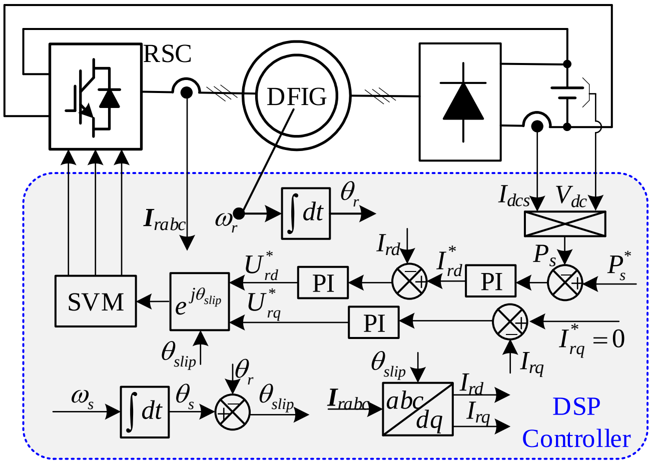

Fig. 1. DFIG-DC system and control diagram of RSC.

III. PERFORMANCE ANALYSIS

When the diode rectifier is conducting, the steady state equivalent circuit of DFIG connected to diode bridge can be seen in Fig. 2. The RSC and rotor side can be equivalent as a current source which is expressed as $\boldsymbol{I}_r$. $\boldsymbol{I}_s$ and $\boldsymbol{I}_m$ represent the stator and exciting current. $\boldsymbol{U}_s$ and $\boldsymbol{E}_m$ represent the stator voltage and air gap voltage, L_m and $L_{s\sigma}$ represent the mutual inductance and stator leakage inductance, R_s represents the stator resistance.

According to the equivalent circuit in Fig. 2, the relationship between stator current and rotor current can be expressed as,

$$\boldsymbol{I}_r = \boldsymbol{I}_s + \boldsymbol{I}_m \tag{4}$$

Since the stator resistance compared with stator leakage inductance is small, it can typically be ignored. Thus, the air gap voltage can be calculated as,

$$\boldsymbol{E}_m = j\omega_s L_m \boldsymbol{I}_m = \boldsymbol{U}_s + j\omega_s L_{s\sigma} \boldsymbol{I}_s \tag{5}$$

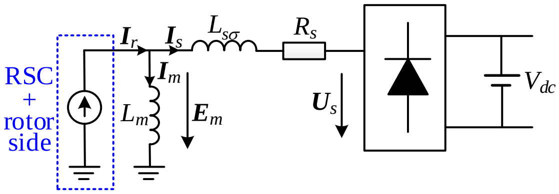

Fig. 2. Steady-state equivalent circuit of the DFIG-DC system.

Since the stator voltage is almost the same phase with stator current due to the characteristic of diode bridge [9], the phasor diagram in steady state can be illustrated in Fig. 3, where δ is the phase angle between stator voltage and rotor current.

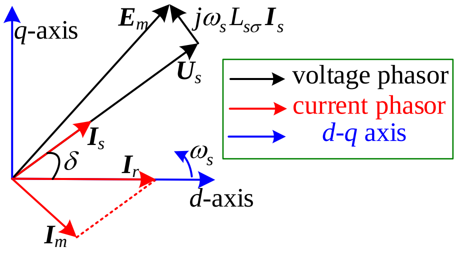

Fig. 3. Phasor diagram of DFIG in steady state.

Combining (4) and (5), the rotor current can be expressed by stator voltage and stator current as,

$$\boldsymbol{I}_r = \boldsymbol{I}_s + \frac{\boldsymbol{U}_s + j\omega_s L_{s\sigma}\boldsymbol{I}_s}{j\omega_s L_m} = \frac{L_s}{L_m}\boldsymbol{I}_s - j\frac{\boldsymbol{U}_s}{\omega_s L_m} \tag{6}$$

where L_s is the stator inductance which is equal to the sum of L_m and $L_{s\sigma}$.

Since the stator current and stator voltage are in phase, $(L_s/L_m)\boldsymbol{I}_s$ and $j\boldsymbol{U}_s/(\omega_s L_m)$ are orthogonal relationship. The angle between the stator current and rotor current is δ, which can be expressed as,

$$\delta = \arctan\left(\frac{|\boldsymbol{U}_s|}{\omega_s L_s |\boldsymbol{I}_s|}\right) \tag{7}$$

The relationship between the rotor current and stator current can be deduced as,

$$\frac{L_s}{L_m}|\boldsymbol{I}_s| = |\boldsymbol{I}_r|\cos\delta \Leftrightarrow |\boldsymbol{I}_s| = \frac{L_m}{L_s}|\boldsymbol{I}_r|\cos\delta \tag{8}$$

Thereby, the stator power can also be expressed by the rotor current as,

$$P_s = |\boldsymbol{U}_s||\boldsymbol{I}_s| = \frac{L_m}{L_s}|\boldsymbol{U}_s||\boldsymbol{I}_r|\cos\delta \tag{9}$$

As can be seen from (9), the stator power is proportional correlation with the magnitude of rotor current, which indicates that the magnitude of rotor current can be used for regulating the stator power. When the stator power is zero, which manifests that the stator current is zero, the stator voltage is the same as the air gap voltage. In this condition, the angle between stator voltage and rotor current is 90 degree, which can be seen from (7). With the increase of stator power, the angle will decrease since the stator current is increasing. Thus, the range of this angle is limited to be between 0 to 90 degree.

As can be seen from (9), the relationship between stator power and magnitude of rotor current is non-linear. It is necessary to build a small signal model to analyze the stability of power control loop. Assuming that the steady state working point is P_{s0} , $\boldsymbol{I}_{r0}$ and δ_0, the small signal of power can be deduced as,

$$\Delta P_s = \frac{L_m}{L_s}\left|\boldsymbol{U}_s\right|\cos\delta_0\Delta\left|\boldsymbol{I}_r\right| - \frac{L_m}{L_s}\left|\boldsymbol{U}_s\right|\left|\boldsymbol{I}_{r0}\right|\sin\delta_0\Delta\delta \qquad (10)$$

It should be noted that angle δ is not an independent variable, which is determined by the stator power P_s. Based on (7) and (9), the relationship between the angle δ and stator power P_s can be expressed as,

$$\Delta\delta = -\frac{L_s}{L_m}\frac{\sin\delta_0}{\left|\boldsymbol{U}_s\right|\left|\boldsymbol{I}_{r0}\right|}\Delta P_s \qquad (11)$$

It can be seen that (11) is not directly obtained from (10) because the derivative from power to angle is different from angle to power.

According to the parameter design principle shown in [5], the outer loop of power control is always designed one tenth of the inner loop of current control. In this letter, the bandwidth of inner loop is designed as 100 Hz and the bandwidth of outer loop is designed as 10 Hz. Based on the DFIG parameters shown in Table I, the proportional and integral gain of the inner current control loop are 6.9 and 553, respectively.

Since the inner loop of rotor current control is much faster than the outer power control loop, it can be simplified as a unity gain block. Also according to (10) and (11), the block diagram of power control loop can be shown as Fig. 4. Based on Fig. 4, the proportional and integral gain of power control loop are 0.1 and 62 when the bandwidth of power control loop is 10 Hz.

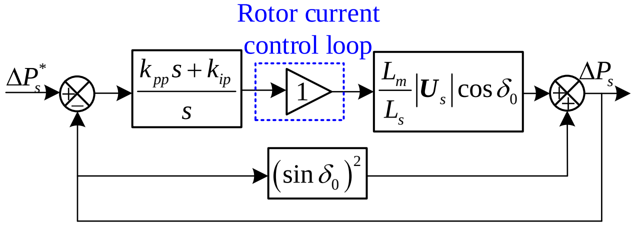

Fig. 4. Block diagram of power control loop.

According to Fig. 4, the transfer function of power control loop can be deduced as,

$$\frac{\Delta P_s}{\Delta P_s^*} = \frac{\frac{L_m}{L_s}\left|\boldsymbol{U}_s\right|\left(k_{pp}s+k_{ip}\right)\Big/\cos\delta_0}{s+\frac{L_m}{L_s}\left|\boldsymbol{U}_s\right|\left(k_{pp}s+k_{ip}\right)\Big/\cos\delta_0} \qquad (12)$$

According to the transfer function of power loop shown in (12), the pole map of stator power changing from zero to 1 pu is plotted in Fig. 5. No matter how much the stator active power is produced, the pole is in the left plane which indicates the power control loop is always stable. Compared with other field-oriented control , the power control loop is reduced to be a first-order system, which eliminates the effect of orientation angle and improve the stability of power control loop.

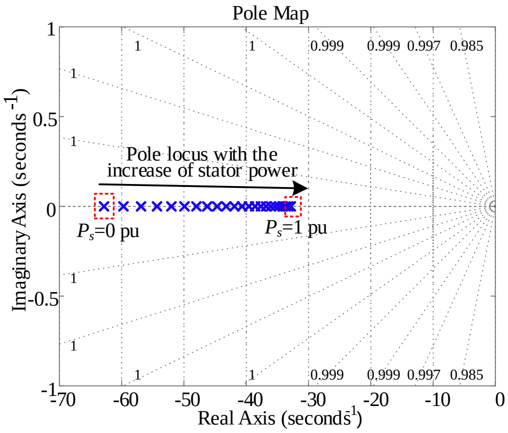

Fig. 5. Pole map of power control loop with stator power changing from 0 to 1 pu.

IV. EXPERIMENTAL RESULTS

In order to validate the proposed control scheme, a DFIG-based experimental system shown in Fig. 6 is developed . The DFIG is driven by an induction motor, which simulates the prime motor. The control strategy of RSC is implemented on the TI TMS320F28335 DSP and the switching frequency is 10 kHz with a sampling frequency of 10 kHz. The parameters of the DFIG are shown in Table I. All the experimental waveforms are acquired by a YOKOGAWA DL750 scope.

TABLE I Parameters of the tested DFIG.

Parameters	*Value*	*Parameters*	*Value*
Rated power	1.0 kW	Rated voltage	110 V
Rated frequency	50 Hz	DC voltage	140 V
Stator/rotor	0.33	R_s	1.01 Ω
R_r	0.88 Ω	L_m	87.5 mH
$L_{\sigma s}$	5.6 mH	$L_{\sigma r}$	5.6 mH

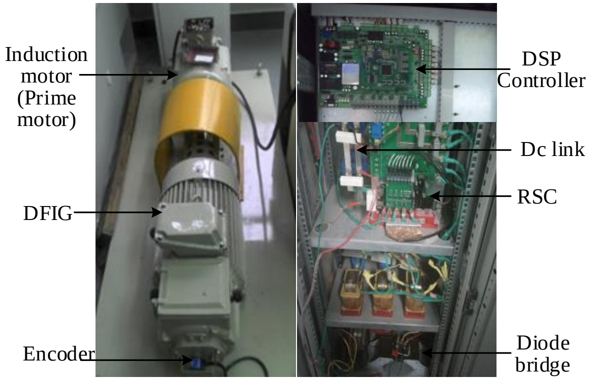

Fig. 6. Experimental set up of DFIG-DC system.

The experimental results of stator flux orientated control in [6] with dc sampling offset in stator voltage is shown in Fig. 7. The stator power reference is 200 W. The stator frequency reference is 50 Hz. In this method, the stator flux angle is calculated based on the integral of stator voltage and the rotor exciting current reference is the output of stator flux angle control loop. The dc sampling offset causes that the rotor exciting current contains 50 Hz pulsation and the envelope of stator current oscillates at 50 Hz. Thus, it is necessary to find some new control method to eliminate the dc sampling offset effect.

This article has been accepted for publication in a future issue of this journal, but has not been fully edited. Content may change prior to final publication. Citation information: DOI 10.1109/TPEL.2019.2953677, IEEE Transactions on Power Electronics

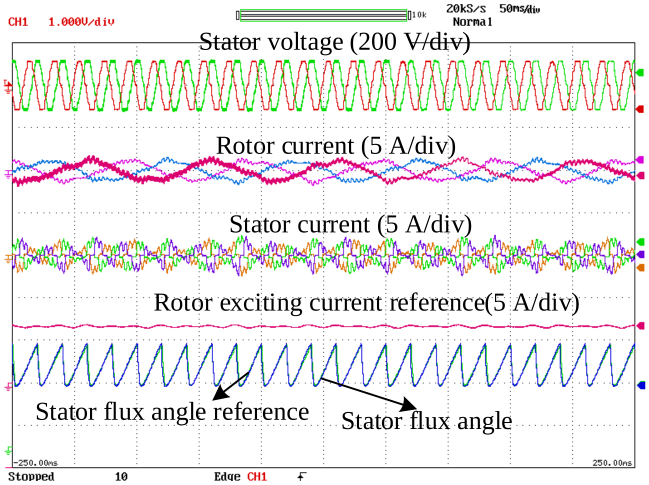

Fig. 7 Experimental results of DFIG using stator flux orientated control with stator voltage and current sensors [6].

Fig. 8 shows the step response of DFIG using the simplified control method when the stator active power reference changes from 200 W to 600 W. The rotor speed is 900 rpm and the stator frequency is set as 50 Hz. The stator active power can track the power reference accurately in 100 ms without steady state error. Compared with Fig. 7, the power ripples only contain 300 Hz component without 50 Hz component which means it can eliminate the dc sampling effect and the parameter dependence.

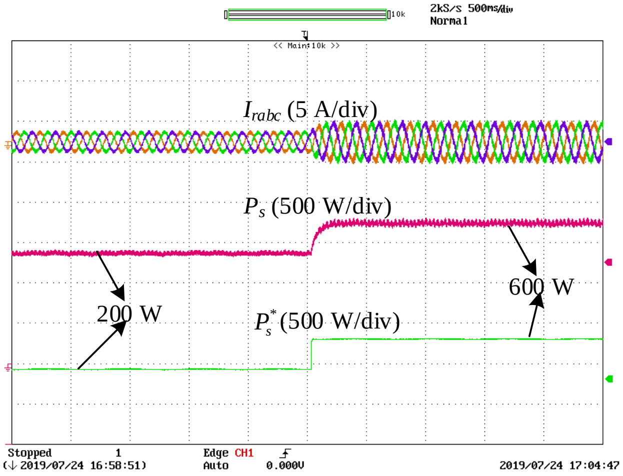

Fig. 8. Step response of stator power change without stator side sensors.

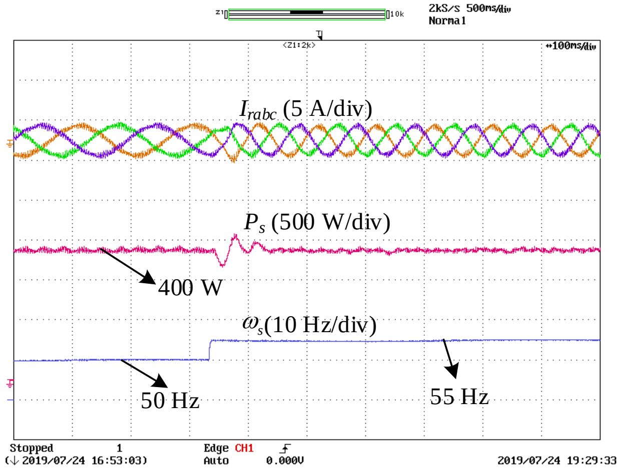

Fig. 9. Step response of stator frequency change without stator side sensors.

Fig. 9 shows the step response of DFIG with the simplified control scheme when the stator frequency change from 50 Hz to 55 Hz. During the change of stator frequency, the stator power has a little pulsation but will come to steady state within 95 ms, which indicates that the power can always be controlled stable even during frequency change.

V. CONCLUSION

This letter proposes a simplified stator frequency and power control method of DFIG-DC system by just regulating rotor current vector. Since only the rotor currents are necessary for the control, the stator voltage and current sensors can both be avoided. Furthermore, the parameter dependency and dc sampling offset question are also eliminated without the voltage model or current model for acquiring the stator flux. In conclusion, this simplified stator frequency and power control method is a highly robust method for the DFIG-DC system.

REFERENCES

[1] M. F. Iacchetti, G. D. Marques, R. Perini, “Operation and Design Issues of a DFIG Stator-Connected to a DC-Net by a Diode Rectifier,” *IET Electric Power Applications*, vol 8, no. 8, pp. 310-319, Sept. 2014.

[2] N. Yu, H. Nian, and Y. Quan, “A novel DC grid connected DFIG system with active filter based on predictive current control,” in *Proc. Int. Conf. Elect. Mach. Syst.*, Aug. 22–23, 2011, pp. 4525–4537

[3] S. Yan, A. Zhang, H. Zhang, and J. Wang, “Control scheme for DFIG converter system based on DC-transmission,” *IET Electr. Power Appl.*, vol. 11, no. 8, pp. 1441–1448, Sep. 2017.

[4] P. Maciejewski and G. Iwanski, “Direct torque control for autonomous doubly fed induction machine based DC generator,” in *Proc. 12th Int. Conf. Ecol. Veh. Renew. Energy*, Monte Carlo, Monaco, 2017, pp. 1–6.

[5] D. Zhou and F. Blaabjerg. “Bandwidth oriented proportional-integral controller design for back-to-back power converters in DFIG wind turbine system,” *IET Renew. Power Gener.*, vol. 11 no. 7, pp. 941-951, 2017.

[6] G. D. Marques and M. F. Iacchetti, “Stator frequency regulation in a field oriented controlled DFIG connected to a DC link,” *IEEE Trans. Ind. Electron.*, vol. 61, no. 11, pp. 5930-5939,Nov. 2014.

[7] G. D. Marques and M. F. Iacchetti, “Inner control method and frequency Regulation of a DFIG Connected to a DC Link,” *IEEE Trans. Energy Convers.*, vol.29, no.2, pp.435-444, Jun. 2014.

[8] M. F. Iacchetti, G. D. Marques, and R. Perini, “Torque ripple reduction in a DFIG-DC system by resonant current controllers,” *IEEE Trans. Power Electron.*, vol. 30, no. 8, pp. 4244–4254, Aug. 2015.

[9] H. Nian, C. Wu, and P. Cheng, “Direct resonant control strategy for torque ripple mitigation of DFIG connected to DC link through diode rectifier on stator,” *IEEE Trans. Power Electron.*, vol. 32, no. 9, pp. 6936–6945, Sep. 2017.

[10] G. D. Marques and M. F. Iacchetti, “A self-sensing stator-current-based control system of a DFIG connected to a DC-link”, *IEEE Trans. on Power Electron.*, Vol. 62, No. 10, pp. 6140-6150, Oct. 2015.

[11] C. Wu and H. Nian, “An Improved Repetitive Control of DFIG-DC System for Torque Ripple Suppression,” *IEEE Trans. on Power Electron.*, vol. 33, no.9, pp. 7634-7644, Sep. 2018.

[12] H. Misra and A. K. Jain, “Analysis of stand alone DFIG-DC system and DC voltage regulation with reduced sensors,” *IEEE Trans Ind. Electron.*, vol. 64, no. 6, pp. 4402–4412, Jun. 2017.

[13] C. Wu and H. Nian, “Sinusoidal current operation of DFIG-DC system without stator voltage sensors,” *IEEE Trans. Ind. Electron.*, vol. 65, no. 8, pp. 6250–6258, Aug. 2018.

[14] K. Xiahou, X. Lin, Y. Liu and Q. H. Wu, "Robust rotor-current sensorless control of doubly fed induction generators," *IEEE Trans. Energy Convers.*, vol. 33, no. 2, pp. 897-899, Jun. 2018.